John L. Volakis
ElectroScience Lab
Elecrical Engineering Dept.
The Ohio State University
1320 Kinnear Rd.
Columbus, OH 43212
+1 (614) 292-5846 Tel.
+1 (614) 292-7297 (Fax)
volakis.1@osu.edu (email)

David B. Davidson
Dept. E&E Engineering
University of Stellencosch
Stellenbosch 7600, South Africa
(+27) 21 808 4458
(+27) 21 808 4981 (Fax)
davidson@ing.sun.ac.za (e-mail)

Foreword by the Editors

The Electric-Field Integral Equation (EFIE) remains one of the stalwarts of Method-of-Moments (MoM) formulations, in particular using the very popular Rao-Wilton-Glisson (RWG) basis functions (now recognized as the lowest-order divergence-conforming element, very closely related to the curl-conforming Whitney edge elements used in Finite Element Method analysis). However, there are a number of potential pitfalls with this technique, in particular the poor matrix condition numbers often encountered when dealing with large problems. Readers may be aware of recent work on "loop-tree" and "loop-star" basis functions, which attempt to provide a partially decoupled basis for the components of the impedance matrix obtained from the vector magnetic and scalar electric potentials. This paper evaluates these basis functions, and compares convergence rates using an iterative solver to results using RWG basis functions. It should be of interest to anyone interested in extending the capabilities of MoM analysis using the electric-field integral equation, and we thank the author for his contribution.

Iterative-Solver Convergence for Loop-Star and Loop-Tree Decompositions in Method-of-Moments Solutions of the Electric-Field Integral Equation

Thomas F. Eibert

FGAN-FHR
Neuenahrer Str. 20, 53343 Wachtberg, Germany
E-mail: eibert@fgan.de

Abstract

Method-of-Moments (MoM) solutions of the electric-field integral equation using Rao-Wilton-Glisson (RWG) basis functions suffer from the so-called low-frequency breakdown. Introduction of loop-tree or loop-star decompositions of the basis functions can effectively solve this problem, and a number of papers have been published discussing various aspects with respect to these techniques. Several papers imply that loop-tree or loop-star decompositions may help to improve iterative-solver convergence for the solution of the resulting linear-equation systems. Since only a few results with respect to this issue are available, a study of the frequency-dependent iterative-solver convergence for RWG, loop-tree, and loop-star basis functions was performed. Two metallic scattering objects, with meshes comprising up to 21060 unknowns, were considered. RWG functions were found to provide the best convergence behavior, as long as the frequency considered was high enough to prevent the low-frequency breakdown. Among the loop-tree and loop-star bases, the loop-tree functions were found to be superior to the loop-star functions. The loop-tree functions resulted in good and stable convergence behavior if the number of subdivisions

per wavelength was larger than a few hundred. Moreover, it is shown that the so-called loop-tree decomposition can also be viewed as a loop-cotree decomposition if an alternative tree of edges connecting the free vertices of the mesh is constructed.

Keywords: Integral equation; electric field integral equation; moment methods; iterative methods; convergence of numerical methods; mesh generation

1. Introduction

Method-of-moments (MoM) solutions of surface integral equations are the preferred numerical methods for the solution of electromagnetic radiation and scattering problems involving metallic and homogeneous objects. Since the pioneering work by Rao, Wilton, and Glisson [1], dealing with arbitrarily shaped metallic objects, most implementations have worked with triangular surface discretizations and the associated Rao-Wilton-Glisson (RWG) basis functions [1]. Also, the mixed-potential integral equation (MPIE) representation of the electric-field integral equation (EFIE) in [1] has become commonplace for the computation of the coupling integrals. Restricting the discussion to metallic objects, the first-kind hypersingular electric-field integral equation is preferably replaced by the second-kind magnetic-field integral equation (MFIE). However, the magnetic-field integral equation is not applicable for open metallic objects, and due to the problem of interior resonances, closed metallic objects are often treated by a linear combination of the electric-field integral equation and the magnetic-field integral equation: the combined-field integral equation (CFIE) [2, 3]. Also, the modeling accuracy of the electric-field integral equation is often superior to the magnetic-field integral equation, especially when objects with sharp edges and corners are involved. A serious problem of the electric-field integral equation is its so-called low-frequency breakdown, which means that a reliable solution cannot be found if the discretization becomes very fine in terms of subdivisions per wavelength. Finer discretizations cause larger matrix condition numbers and, eventually, the breakdown of the solution. When iterative equation solvers are employed, the increasing condition number requires decreasing residual errors to achieve accurate solutions. Recently, analytically preconditioned versions of the electric-field integral equation have been developed [4]. However, currently available numerical implementations require considerably more computational resources than those for the conventional electric-field integral equation.

Another solution to the low-frequency breakdown of the electric-field integral equation is given by loop-star or loop-tree decompositions of the RWG basis functions. These techniques were introduced in the early 1980s [5, 6], and utilize the fact that electric and magnetic fields decouple for decreasing frequencies. The basic idea is to introduce divergence-free loop functions, and to extend the solution space of the loop functions by a second set of functions such that the solution space of the original RWG functions is retained. Thus, an incomplete Hodge decomposition [7] (similar to the well-known Helmholtz decomposition of vector fields) of the surface currents is realized, and a well-behaved MoM equation system is obtained for decreasing frequencies, provided that the matrix entries are appropriately scaled.

Very detailed studies of loop-star and loop-tree decompositions are to be found in [8] and [9]. The results on matrix condition numbers in [8] are interesting. Both loop-star and loop-tree decompositions resulted in almost frequency-independent condition numbers. However, the loop-star condition number was found to be more than an order of magnitude larger than that of the loop-tree decomposition (more than 10000, as compared to about 1000). In contrast to this, the loop-star condition numbers in [9] were about 1000, which might have been due to the razor-blade testing, as opposed to the usual Galerkin technique, used in [8]. Also, [9] provided results on the diagonal dominance ratio (DDR) of the coupling matrix resulting from loop-star decompositions. Since the diagonal dominance ratio for the loop-star decomposition is typically better than for RWG functions, it is expected that the loop-star equation system will be more amenable to iterative solvers.

In [10], the loop-star functions were applied to the analysis of microstrip antennas, and it was found that the resulting formulation was robust for the entire frequency range of interest. [11] discussed the relationship between isotropic scalar quantities and loop-star functions, and also implied that the improved diagonal dominance ratio resulting from the loop-star functions may help with iterative solvers. Results on iterative-solver convergence for a relatively low frequency were given in [12]. The authors found that the equation systems for loop-star and loop-tree decompositions still exhibited bad convergence behavior, which was due to the star or tree basis functions. As a remedy to this issue, a second basis-function rearrangement was introduced that projected the star or tree functions on pulse basis functions for electric charges. Unfortunately, the resulting matrix deteriorated for increasing frequencies. In [13], loop-star basis functions were employed in preconditioned iterative solutions of electric-field integral-equation scattering problems. Results were given for a very high frequency (only five subdivisions per wavelength), and it was implied that the loop-star decomposition helped to improve iterative-solver convergence. Since no comparison with RWG functions was included, it is not easy to quantify the results given, and it is also doubtful whether the iteration numbers for a residual error of 0.01 (to be compared to a matrix condition number larger than 10000) were of any practical relevance.

The purpose of the present contribution is to compare dependence on frequency of the iterative-solver convergence behavior of loop-star, loop-tree, and RWG functions. It is certainly clear that loop-tree and loop-star functions are superior to RWG functions for low frequencies. However, one may still wonder whether iterative-solver convergence improvement can be expected in the popular MoM frequency ranges with about 10 subdivisions per wavelength. Before convergence results for scattering applications are presented, a short review of some basic equations is given. It is shown that the loop-tree decomposition can also be interpreted as a loop-cotree decomposition, related to the tree-cotree techniques in Finite-Element Methods [14, 15].

2. Formulation

Consider a time-harmonic (time factor $e^{j\omega t}$) surface integral-equation technique using the electric-field integral equation in a mixed-potential integral-equation formulation for metallic objects. According to [1], a Galerkin-type MoM equation system is derived as

$$[Z_{mn}]\{I_n\} = \{b_m\}, \quad m,n = 1,...,N, \tag{1}$$

where the I_n are the unknown surface-current expansion coefficients, the b_n are the excitation vector elements due to an incident wave or delta-gap voltage sources, and N is the number of unknowns. The MoM matrix elements are given by

$$Z_{mn} = Z_{mn}^{A} + Z_{mn}^{\phi}, \tag{2}$$

with

$$Z_{mn}^{A} = -j\frac{\omega\mu}{4\pi}\int_A\int_A\left[\mathbf{f}_m(\mathbf{r})\cdot\bar{\mathbf{I}}\frac{e^{-jk|\mathbf{r}-\mathbf{r}'|}}{|\mathbf{r}-\mathbf{r}'|}\cdot\mathbf{f}_n(\mathbf{r}')\right]da'da\,, \tag{3}$$

$$Z_{mn}^{\phi} = j\frac{\omega\mu}{4\pi k^2}\int_A\int_A\left\{\left[\nabla\cdot\mathbf{f}_m(\mathbf{r})\right]\frac{e^{-jk|\mathbf{r}-\mathbf{r}'|}}{|\mathbf{r}-\mathbf{r}'|}\left[\nabla'\cdot\mathbf{f}_n(\mathbf{r}')\right]\right\}da'da\,. \tag{4}$$

$\bar{\mathbf{I}}$ is the unit dyad, and k is the wavenumber in the medium considered. Also, $\mathbf{f}_n$ and $\mathbf{f}_m$ are Rao-Wilton-Glisson expansion and testing functions, respectively [1], and A is the surface of the scattering or radiation object. The reason for the low-frequency breakdown is the different frequency scaling of Equations (3) and (4) (k is proportional to ω). For decreasing ω, the contribution of the also decreasing magnetic vector potential contribution, Equation (3) (as compared to the electric scalar potential contribution, Equation (4)) is eventually no longer captured by finite computer accuracy. If one uses a discretization with about 10 subdivisions per wavelength, the condition number of the resulting equation system is typically smaller than 100, but increases badly if the mesh becomes finer (see [8] for quantitative results).

A solution to this problem is found if it is possible to decouple the contributions of Equations (3) and (4), for instance, by the construction of an appropriate set of basis functions. Ideally, we wish to have two types of basis functions: one contributing to Equation (3) only, and the other one contributing to Equation (4) only. In this case, we would have to solve two separate (smaller and better-behaved) equation systems for the two types of basis functions. However, this is possible only for vanishing ω, when electric and magnetic fields are decoupled. Nevertheless, one can try to decouple Equations (3) and (4) as well as possible, and this is achieved by the so-called Hodge decomposition of the surface-current densities. That is, the surface currents are split into curl-free and divergence-free contributions. Using the RWG basis as a starting point, only an incomplete Hodge decomposition can be realized. However, this is sufficient to remove the low-frequency breakdown.

The loop functions are constructed as a linear combination of RWG functions, such that they are divergence-free. For a simply-connected surface mesh, as illustrated in Figure 1, we introduce one loop function for every free vertex in the mesh (indicated by the bold dots in Figure 1) by linearly combining all RWG functions corresponding to all edges connected at the vertex (see the circular arrows in the figure). If we first construct a complete tree of edges connecting all free vertices of the mesh (see the bold edges in Figure 1), we can easily integrate the loop-tree or loop-star decomposition into an existing MoM code working with RWG functions. For every loop function introduced, we just delete one RWG function for a tree edge. Doing this, the so-called loop-tree decomposition has been finished just by introducing the loop-functions. According to this procedure, the loop-tree decomposition can also be called a loop-cotree decomposition, since we retain the RWG functions on the cotree. This procedure is strongly related to the tree-cotree techniques introduced in the finite-element community [14, 15]. Alternatively, another tree can be constructed connecting the centroids of the mesh triangles (see the fine lines in Figure 1). Using such a tree, our cotree edges can also be identified as the edges crossed by the branches of this new tree [8].

In contrast to this, the star functions are related to the mesh triangles (one star function for all triangles but one in simply-connected meshes, as shown in Figure 1). They are constructed by linearly combining all RWG basis functions defined on a triangle such that the surface charges on the triangle add. Further details on

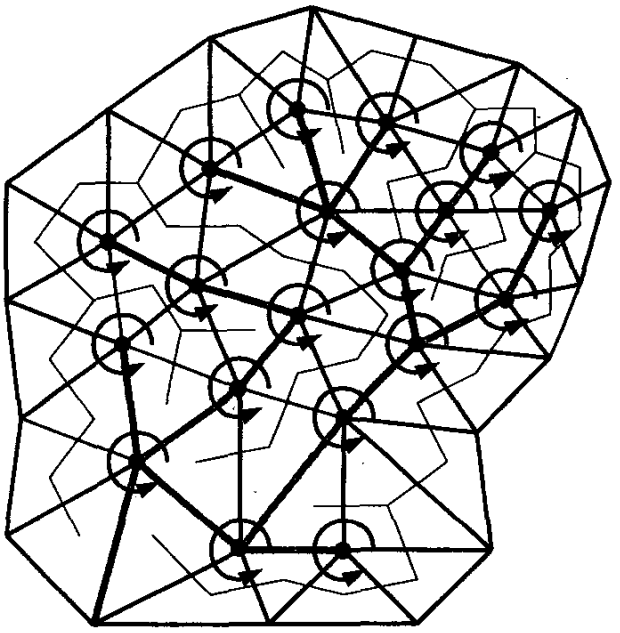

Figure 1. A triangular mesh for discretizing the electric-field integral equation. The dark dots indicate free vertices, representing the centers of loop basis functions illustrated by the circular arrows. Bold edges span a tree connecting the free vertices, and the fine lines span an alternative tree, connecting the centroids of all triangles.

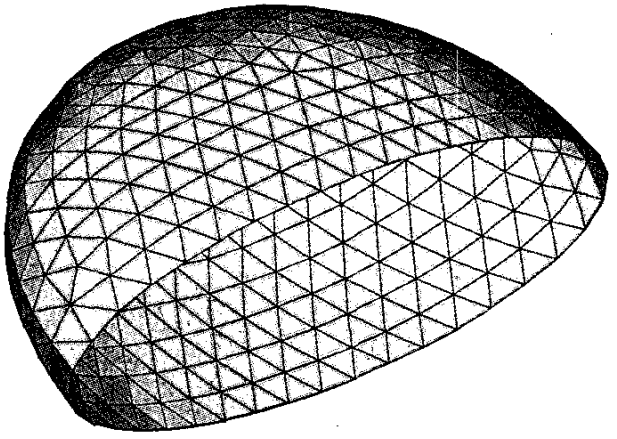

Figure 2. The geometry and mesh of a metallic half-ellipsoid shell. The surface normal of the opening is directed along $-y$, and the x-polarized incident plane wave propagates in the $-z$ direction. The number of unknowns is 1003 for all sets of basis functions.

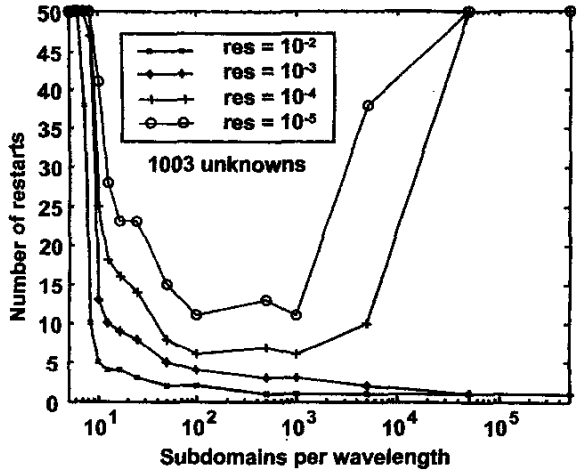

Figure 3. The convergence behavior of GMRES(10) as a function of frequency for the problem in Figure 2 using RWG basis functions (1003 unknowns).

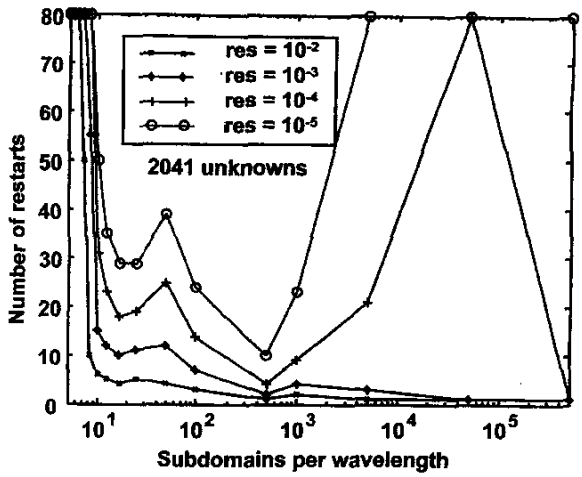

Figure 6. The convergence behavior of GMRES(10) as a function of frequency for the problem in Figure 2 using RWG basis functions (2041 unknowns).

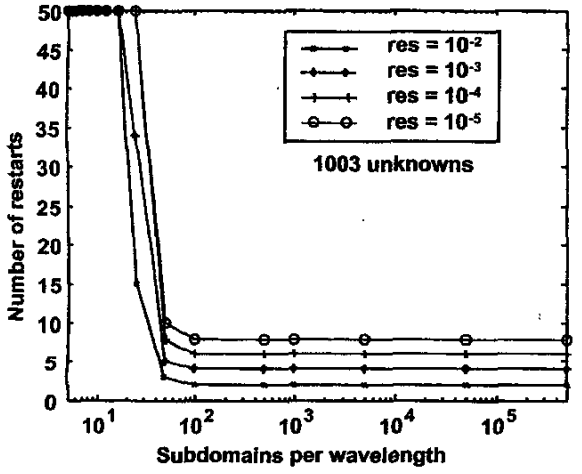

Figure 4. The convergence behavior of GMRES(10) as a function of frequency for the problem in Figure 2 using loop-tree basis functions (1003 unknowns).

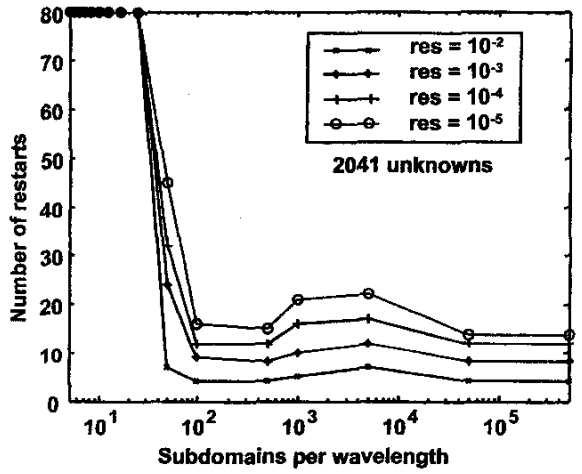

Figure 7. The convergence behavior of GMRES(10) as a function of frequency for the problem in Figure 2 using loop-tree basis functions (2041 unknowns).

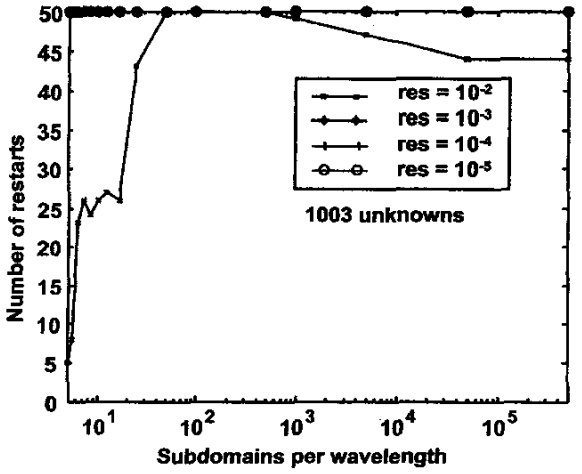

Figure 5. The convergence behavior of GMRES(10) as a function of frequency for the problem in Figure 2 using loop-star basis functions (1003 unknowns).

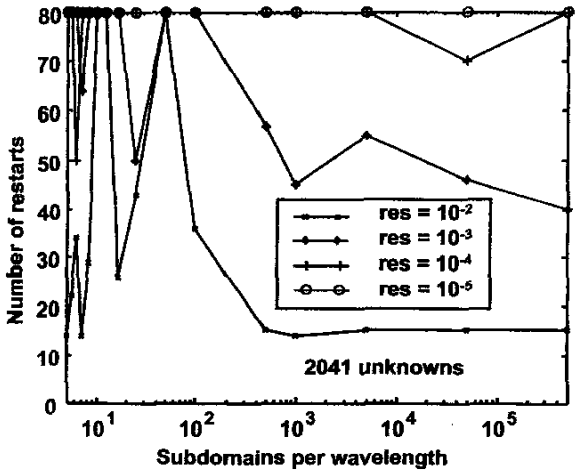

Figure 8. The convergence behavior of GMRES(10) as a function of frequency for the problem in Figure 2 using loop-star basis functions (2041 unknowns).

implementing loop-tree and loop-star decompositions may be found in [8, 9, 13]. The divergence-free property of the loop functions is essential for loop-tree and loop-star decompositions. Thus, the loop functions do not contribute to Equation (4), and the different frequency behaviors of Equations (3) and (4) can be compensated for by appropriate frequency scaling (see [12] for a very detailed discussion).

3. Numerical Results

The purpose of this section is to investigate the frequency-dependent convergence behavior of loop-tree and loop-star decompositions compared to RWG functions, when the resulting equation system is solved by an iterative solver. We considered two different metallic scattering objects, and chose the generalized minimal residual (GMRES) iterative solver (restarted version, with n search vectors in GMRES(n)), since it produces a smooth residual error. The matrix elements were normalized such that the diagonal elements were of the same order of magnitude, and a simple Jacobi-like preconditioner was applied. The first example was the half-ellipsoid metallic shell shown in Figure 2. A computation of the matrix condition number for a mesh with 536 unknowns gave results similar to those found in [8]. RWG functions resulted in a small condition number (less than 100) for about 10 subdivisions per wavelength or less, but caused – with power of two – increasing condition numbers for larger numbers of subdivisions per wavelength. The loop-tree decomposition resulted in a constant condition number of about 900, and the loop-star decomposition caused a constant condition number of about 40000. Since larger condition numbers typically require smaller residual solver errors, we should keep these observations in mind when we judge the solver convergence results. Figures 3 to 8 give the convergence results for RWG, loop-tree, and loop-star basis functions, as a function of the approximate number of subdivisions per wavelength. Two different meshes were considered: one with 1003 unknowns (shown in Figure 2) and one with 2041 unknowns. The varying numbers of subdivisions or subdomains per wavelength were realized by varying the frequency. The excitation was an incident plane wave, propagating towards the opening of the ellipsoid shell. RWG functions required increasing numbers of iterations for a smaller number of subdivisions per wavelength; in particular, less than 10 subdivisions per wavelength needed many iterations. Despite increasing condition number, increasing numbers of subdivisions required less iterations. For more than about 1000 subdivisions per wavelength, the bad conditioning prevented achieving the low residual errors that would be necessary for correct results.

In case of loop-tree decomposition, it was difficult to achieve convergence for small numbers of subdivisions per wavelength. However, for large numbers of subdivisions the equation systems were reliably solved with a constant number of iterations. Unfortunately, we needed more than 100 subdivisions per wavelength in order to achieve the low number of iterations. Consequently, the loop-tree decomposition is not advantageous for "high-frequency" problems where we wish to work with about 10 subdivisions per wavelength or even less. For the loop-star decomposition, we found it difficult to obtain reasonable convergence with the restarted GMRES(10) at all. Interestingly, convergence improved for very low numbers of subdivisions per wavelength (less than 10). This may be the reason why only five subdomains per wavelength were used in [13]. As expected, the problem with the larger number of unknowns required larger numbers of iterations, whereas the typical behavior with respect to frequency remained the same.

In order to investigate the convergence behavior for even larger problems, we considered the corner reflector illustrated in Figure 9. The mesh comprised 21060 unknowns. To efficiently solve this problem, we employed a diagonalized version (high-frequency) of the Multilevel Fast Multipole Method (MLFMM) [16]. Since direct application of MLFMM to the loop-tree or loop-star basis functions is not recommended, due to the large spatial support of these functions, we implemented the MLFMM solver

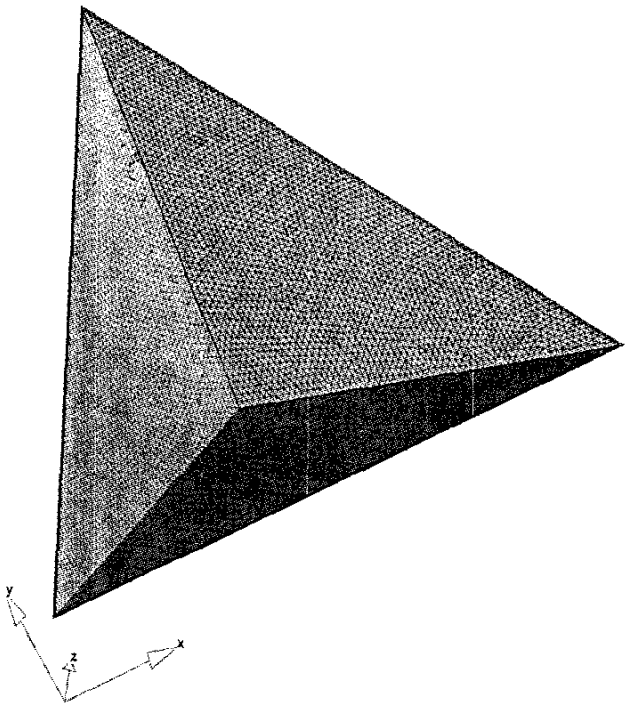

Figure 9. The geometry and mesh of a metallic corner reflector with a side length of 1 m and 21060 unknowns. The y-polarized incident plane wave propagated in the $-z$ direction.

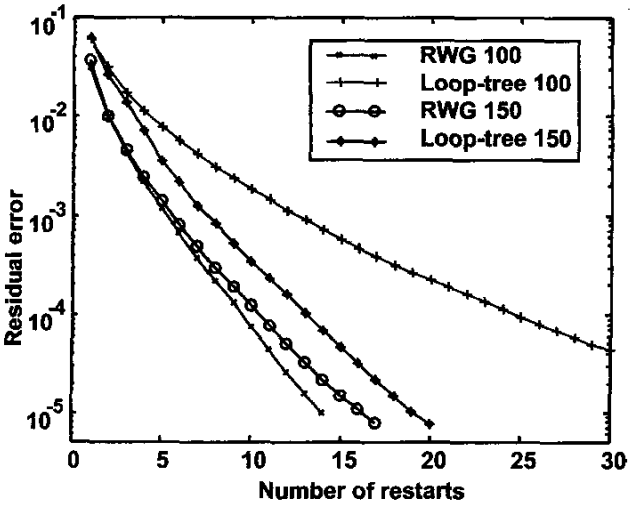

Figure 10. The convergence behavior of GMRES(40) for the problem in Figure 9 using RWG and loop-tree basis functions. The curves with 100 subdivisions per wavelength correspond to $f = 1.875$ MHz, and 150 subdivisions correspond to $f = 1.25$ MHz.

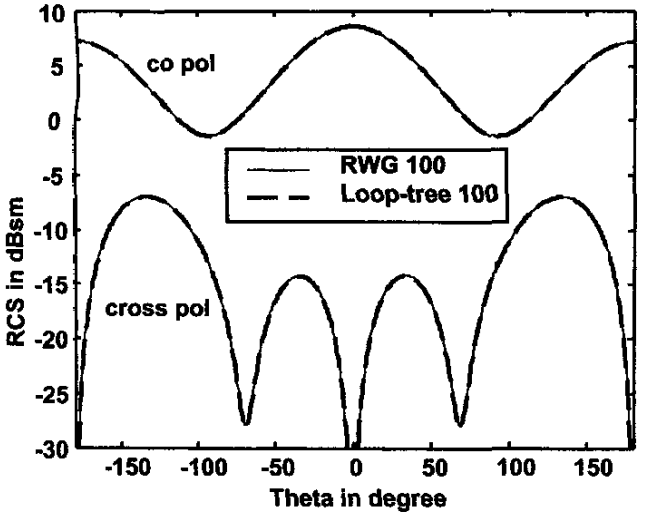

Figure 11. The bistatic radar cross section (RCS) in the *xz* plane for the problem in Figure 9 ($f = 1.875$ MHz) using RWG and loop-tree bases.

using RWG functions, only. Thus, for the evaluation of the MLFMM contributions for the loop-tree and loop-star functions, sparse transformations between the different bases were performed (see also [16]). Convergence results for RWG and loop-tree functions are given in Figure 10 for about 100 and 150 subdivisions per wavelength. RWG convergence was found to be better in both cases. However, loop-tree convergence came close to the RWG rate for 150 subdivisions per wavelength. Figure 11 shows excellent agreement for bistatic radar cross section (RCS) results obtained with RWG and loop-tree bases.

4. Conclusions

The frequency-dependent iterative solver convergence behavior for RWG, loop-tree, and loop-star basis functions in MoM solutions of the electric-field integral equation was investigated, using a restarted GMRES solver. RWG bases were found to be the preferred choice, as long as the number of subdivisions per wavelength was small enough to prevent the well-known low-frequency breakdown. Loop-tree bases were found to behave considerably better than loop-star bases. The loop-tree functions provided for good and stable convergence behavior if the number of subdivisions per wavelength was larger than a few hundred per wavelength. However, convergence was found to be very poor in the "high-frequency" range of about 10 subdivisions per wavelength or less. Moreover, it was shown that the loop-tree basis can also be considered to be a loop-cotree basis if a complete tree of edges connecting the free vertices of the mesh is constructed.

5. References

1. S. M. Rao, D. R. Wilton, and A. W. Glisson, "Electromagnetic Scattering by Surfaces of Arbitrary Shape," *IEEE Transactions on Antennas and Propagation*, **AP-30**, 3, May 1982, pp. 409-418.

2. J. R. Mautz and R. F. Harrington, "H-Field, E-Field, and Combined-Field Solutions for Conducting Bodies of Revolution," *AEÜ*, **32**, 4, 1978, pp. 157-164.

3. A. F. Peterson, "The Interior Resonance Problem Associated with Surface Integral Equations of Electromagnetics: Numerical Consequences and a Survey of Remedies," *Electromagnetics*, **10**, 1990, pp. 293-312.

4. H. Contopanagos, B. Dembart, M. Epton, J. J. Ottusch, V. Rokhlin, J. L. Visher, and S. M. Wandzura, "Well-Conditioned Boundary Integral Equations for Three-Dimensional Electromagnetic Scattering," *IEEE Transactions on Antennas and Propagation*, **AP-S50**, 12, December 2002, pp. 1824-1830.

5. D. R. Wilton and A. W. Glisson, On Improving the Electric Field Integral Equation at Low Frequencies," *USNC/URSI National Radio Science Meeting Digest*, Los Angeles, CA, June 1981, p. 24.

6. J. Mautz and R. F. Harrington, "An E-Field Solution for a Conducting Surface Small or Comparable to the Wavelength," *IEEE Transactions on Antennas and Propagation*, **AP-32**, 4, April 1984, pp. 330-339.

7. R. Leis, *Initial Boundary Value Problems in Mathematical Physics*, Teubner, Stuttgart, 1986.

8. W.-L. Wu, A. W. Glisson, and D. Kajfez, "A Study of Two Numerical Solution Procedures for the Electric Field Integral Equation at Low Frequency," *ACES Journal*, **10**, 3, 1995, pp. 69-80.

9. M. Burton and S. Kashyap, "A Study of a Recent Moment-Method Algorithm that is Accurate to Very Low Frequencies," *ACES Journal*, **10**, 3, 1995, pp. 58-68.

10. S. Uckun, T. K. Sarkar, S. M. Rao, and M. Salazar-Palma, "A Novel Technique for Analysis of Electromagnetic Scattering from Microstrip Antennas of Arbitrary Shape," *IEEE Transactions on Microwave Theory and Techniques*, **MTT-47**, 2, February 1997, pp. 339-346.

11. G. Vecchi, "Loop-Star Decomposition of Basis Functions in the Discretization of the EFIE," *IEEE Transactions on Antennas and Propagation*, **AP-47**, 2, February 1999, pp. 339-346.

12. J.-S. Zhao and W. C. Chew, "Integral Equation Solution of Maxwell's Equations from Zero Frequency to Microwave Frequencies," *IEEE Transactions on Antennas and Propagation*, **AP-48**, 10, October 2000, pp. 1635-1645.

13. J.-F. Lee, R. Lee, and R. J. Burkholder, "Loop Star Basis Functions and a Robust Preconditioner for EFIE Scattering Problems," *IEEE Transactions on Antennas and Propagation*, **AP-51**, 8, August 2003, pp. 1855-1863.

14. D. K. Sun, J. Manges, X. Yuan, and Z. J. Cendes, "Spurious Modes in Finite Element Methods," *IEEE Antennas and Propagation Magazine*, **37**, October 1995, pp. 12-24.

15. S.-C. Lee, J.-F. Lee and R. Lee, "Hierarchical Vector Finite Elements for Analyzing Waveguiding Structures," *IEEE Transactions on Microwave Theory and Techniques*, **MTT-51**, 8, August 2003, pp. 1897-1905.

16. W. C. Chew, J.-M. Jin, E. Michielssen, and J. Song, *Fast and Efficient Algorithms in Computational Electromagnetics*, Boston, Artech House, 2001.